Numerical Conformal Mapping onto the Exterior Unit Disk with a Straight Slit and Logarithmic Spiral Slits

IOP Conf. Series: Journal of Physics: Conf. Series **1212** (2019) 012015 doi:10.1088/1742-6596/1212/1/012015

Numerical Conformal Mapping onto the Exterior Unit Disk with a Straight Slit and Logarithmic Spiral Slits

Ali H.M. Murid[1], Arif A.M. Yunus[2], Mohamed .M.S. Nasser[3]

[1]Department of Mathematical Sciences, Faculty of Science, Universiti Teknologi Malaysia, 81310 Johor Bahru, Johor, Malaysia

[2]Faculty of Science and Technology, Universiti Sains Islam Malaysia, 71800 Bandar Baru Nilai, Nilai, Negeri Sembilan, Malaysia

[3]Department of Mathematics, Statistics and Physics, Qatar University, P.O. Box: 2713, Doha, Qatar

E-mail: alihassan@utm.my; arifasraf@usim.edu.my; mms.nasser@qu.edu.qa

Abstract. This paper presents a fast boundary integral equation method for numerical conformal mapping of unbounded multiply connected regions onto a disk with an infinite straight slit and finite logarithmic spiral slits. Some numerical examples are given to show the effectiveness of the proposed method.

1. Introduction

Conformal mapping is an important tool to solve several problems in the fields of science and engineering [1]. Since exact conformal maps are known only for some regions, numerical methods for computing conformal mappings are highly demanded.

For the conformal mappings of multiply connected regions, several canonical slit regions are available. Thirty nine of these canonical regions have been catalogued by Koebe in his classical paper [2]. These canonical regions have been divided into five categories. For the first four categories, the special points (points to be mapped to 0 or ∞) are chosen in the interior of the region. For the fifth category, the special points are chosen on the boundary.

Several numerical methods have been proposed for computing the conformal mapping of multiply connected regions onto the canonical slit regions [3]. In comparison, the approach based on the boundary integral equation with the generalized Neumann kernel can be used for a wide range of canonical slit regions [4, 5, 6, 7, 8, 9]. The numerical computing of conformal mappings from bounded multiply connected regions onto Koebe's fifth category canonical slit regions using the boundary integral equation with the generalized Neumann kernel has been presented in [6]. The method presented in [6] will be extended in this paper to unbounded multiply connected regions. Further, the canonical region consider in this paper is slightly different from the canonical regions considered in [6].

Let G be an unbounded multiply connected region of connectivity $m > 1$ in the extended complex plane $\overline{\mathbb{C}}$. The boundary $\Gamma := \partial G$ consists of m smooth Jordan curves Γ_j, $j = 1, 2, \ldots, m$. We assume that the boundary Γ_1 is the unit circle $|z| = 1$. The orientation of Γ is such that G is always on the left of Γ.

In this paper, we present a numerical method for computing the conformal mapping $w = \omega(z)$ onto the following two types of canonical regions:

(i) The region Ω_1 which is the unbounded region in the exterior of the unit circle $|w| = 1$ with an infinite straight slit on the line $\operatorname{Im} w = 0$ and $m-2$ finite spiral slits (see Figure 1 (left) for $m = 5$).

(ii) The region Ω_2 which is the unbounded region in the exterior of the unit circle $|w| = 1$ with a semi-infinite straight slit on the line $\operatorname{Im} w = 0$ and $m-2$ finite spiral slits (see Figure 1 (right) for $m = 5$).

Figure 1. The canonical regions Ω_1 (left) and Ω_2 (right).

We assume that the mapping function $w = \omega(z)$ maps the unit circle Γ_1 onto the infinite straight slit for the case of Ω_1 and onto the semi-infinite straight slit for the case of Ω_2. For both cases, we assume that $w = \omega(z)$ maps the curve Γ_2 onto the unit circle $|w| = 1$ and maps the curves Γ_j for $j = 3, 4, \ldots, m$ onto the logarithmic spiral slits $\operatorname{Im}\left[e^{-\mathrm{i}\theta_j} \log w\right] = R_j$, where each θ_j is the angle of intersection between the spiral and any arbitrary ray issuing from the origin. The angle θ_j is called the "oblique angle" of the slit. The logarithmic spiral degenerates into a ray issuing from the origin for $\theta_j = 0$ and degenerates to a circle with center at the origin for $\theta_j = \pi/2$. The real constants R_j for $j = 3, 4, \ldots, m$ are unknown and should be determined in the process of computing the conformal mapping. Thus, the mapping function ω satisfies the boundary conditions

$$\begin{aligned} \operatorname{Im} \omega(\zeta) &= 0, \quad \zeta \in \Gamma_1, && (1)\\ |\omega(\zeta)| &= 1, \quad \zeta \in \Gamma_2, && (2)\\ \operatorname{Im}\left[e^{-\mathrm{i}\theta_j} \log \omega(\zeta)\right] &= R_j, \quad \zeta \in \Gamma_j, \quad j = 3, \ldots, m. && (3) \end{aligned}$$

2. The generalized Neumann kernel

Suppose that each curve Γ_j is parametrized by a 2π-periodic twice continuously differentiable complex function $\eta_j(t)$ with non-vanishing first derivative. Let the total parameter domain J be the disjoint union of the m intervals $J_1, \ldots, J_m$. We define a parametrization η of the whole boundary Γ on J by

$$\eta(t) = \begin{cases} \eta_1(t), & t \in J_1 = [0, 2\pi], \\ \quad \vdots & \\ \eta_m(t), & t \in J_m = [0, 2\pi]. \end{cases} \tag{4}$$

Let $\theta(t)$ be a piecewise constant function defined on J by

$$\theta(t) = \begin{cases} 0, & t \in J_1 = [0, 2\pi], \\ \pi/2, & t \in J_2 = [0, 2\pi], \\ \theta_3, & t \in J_3 = [0, 2\pi], \\ \quad \vdots & \\ \theta_m, & t \in J_m = [0, 2\pi], \end{cases} \tag{5}$$

where θ_j for $j = 3, \ldots, m$ are given real numbers representing the oblique angles of the spiral slits. For simplicity, such piecewise constant function will be denoted by

$$\theta(t) = (0, \pi/2, \theta_3, \ldots, \theta_m). \tag{6}$$

We define a complex function $A(t)$ for all $t \in J$ by

$$A(t) = e^{\mathrm{i}(\pi/2 - \theta(t))}. \tag{7}$$

Then the generalized Neumann kernel $N(s,t)$ formed with A and η is defined by [10, 11]

$$N(s,t) = \frac{1}{\pi} \operatorname{Im}\left(\frac{A(s)}{A(t)} \frac{\eta'(t)}{\eta(t) - \eta(s)}\right). \tag{8}$$

The kernel $N(s,t)$ is continuous. Closely related to the generalized Neumann kernel is the singular kernel $M(s,t)$ defined by

$$M(s,t) = \frac{1}{\pi} \operatorname{Re}\left(\frac{A(s)}{A(t)} \frac{\eta'(t)}{\eta(t) - \eta(s)}\right). \tag{9}$$

Hence the integral operator $\mathbf{N}\mu(s) := \int_J N(s,t)\mu(t)dt$, $s \in J$, is a Fredholm integral operator and the operator $\mathbf{M}\mu(s) := \int_J M(s,t)\mu(t)dt$, $s \in J$, is a singular integral operator. Both operators are bounded on the space H of real Hölder continuous function on the boundary Γ and map H onto itself. For more details, we refer the reader to [11].

Theorem 1 ([5]) *For a given function $\gamma \in H$, the boundary integral equation*

$$(\mathbf{I} - \mathbf{N})\mu = -\mathbf{M}\gamma \tag{10}$$

has a unique solution μ and the function h given by

$$h = [\mathbf{M}\mu - (\mathbf{I} - \mathbf{N})\gamma]/2 \tag{11}$$

is piecewise constant on the boundary Γ. Further, the function $f(z)$ with the boundary values

$$Af = \gamma + h + \mathrm{i}\mu \tag{12}$$

is analytic in G with $f(\infty) = 0$.

3. The conformal mappings

In this section, we present a numerical method for computing the conformal mapping onto the two canonical regions Ω_1 and Ω_2. However, we need to introduce first the following auxiliary function Φ,

$$w = \Phi(z) = \frac{1}{2}\left(z + \frac{1}{z}\right) = \frac{z^2 + 1}{2z}, \tag{13}$$

which maps the unit circle $|z| = 1$ onto the finite straight slit $\{w : |\operatorname{Re} w| \leq 1,\ \operatorname{Im} w = 0\}$. The function Φ also conformally maps the exterior of the unit circle onto the exterior of this finite straight slit with $\Phi(\infty) = \infty$.

3.1. The region Ω_1

For the function Φ defined by (13), the function Ψ defined by

$$w = \Psi(z) = \frac{1}{\Phi(z)} = \frac{2z}{z^2+1}$$

maps the unit circle $|z| = 1$ onto the infinite straight slit $\{w : |\operatorname{Re} w| \geq 1,\ \operatorname{Im} w = 0\}$; and also conformally maps the exterior of the unit circle onto the exterior of this infinite straight slit with $\Psi(\infty) = 0$ and $\Psi(\pm\mathrm{i}) = \infty$. Let the function γ be defined by

$$\gamma(t) = \begin{cases} 0, & t \in J_1, \\ -\log|(\eta_2(t)-\alpha)\Psi(\eta_2(t))|, & t \in J_2, \\ \operatorname{Im}\left[e^{-\mathrm{i}\theta_j}\log\left((\eta_j(t)-\alpha)\Psi(\eta_j(t))\right)\right], & t \in J_j, \quad j = 3,4,\ldots,m, \end{cases} \tag{14}$$

where α is a given point in the interior of Γ_2. Let also the function μ be the unique solution of the integral equation (10), the function $h = (h_1, h_2, \ldots, h_m)$ be given by (11), and the function f be the analytic function in G with the boundary values (12). Then the function ω defined in G by

$$\omega(z) = (z-\alpha)\Psi(z)e^{f(z)+\mathrm{i}h_1-h_2} \tag{15}$$

is the conformal mapping from the region G onto the canonical region Ω_1. The function ω satisfies the boundary conditions (1)–(3) with $R_j = -h_j + \operatorname{Im}\left[(\mathrm{i}h_1 - h_2)e^{-\mathrm{i}\theta_j}\right]$ for $j = 3,4,\ldots,m$.

3.2. The region Ω_2

For the function Φ defined by (13), the function

$$1 - \Phi(z) = 1 - \frac{z^2+1}{2z} = -\frac{(z-1)^2}{2z}$$

maps the unit circle $|z| = 1$ onto the finite straight slit $\{w : 0 \leq \operatorname{Re} w \leq 2,\ \operatorname{Im} w = 0\}$. Hence, the function Υ defined by

$$w = \Upsilon(z) = \frac{1}{1-\Phi(z)} = -\frac{2z}{(z-1)^2}$$

maps the unit circle $|z| = 1$ onto the semi-infinite straight slit $\{w : \frac{1}{2} \leq \operatorname{Re} w,\ \operatorname{Im} w = 0\}$; and also conformally maps the exterior of the unit circle onto the exterior of this semi-infinite straight slit with $\Upsilon(\infty) = 0$ and $\Upsilon(1) = +\infty + 0\mathrm{i}$. Then, we define a real function γ by

$$\gamma(t) = \begin{cases} 0, & t \in J_1, \\ -\log|(\eta_2(t)-\alpha)\Upsilon(\eta_2(t))|, & t \in J_2, \\ \operatorname{Im}\left[e^{-\mathrm{i}\theta_j}\log\left((\eta_j(t)-\alpha)\Upsilon(\eta_j(t))\right)\right], & t \in J_j, \quad j = 3,4,\ldots,m, \end{cases} \tag{16}$$

where α is a given point in the interior of Γ_2. Let the function μ be the unique solution of the integral equation (10), the function $h = (h_1, h_2, \ldots, h_m)$ be given by (11), and the function f be the analytic function in G with the boundary values (12). Then the function ω defined in G by

$$\omega(z) = (z-\alpha)\Upsilon(z)e^{f(z)+\mathrm{i}h_1-h_2} \tag{17}$$

is the conformal mapping from the region G onto the canonical region Ω_1. The function ω satisfies the boundary conditions (1)–(3) with $R_j = -h_j + \operatorname{Im}\left[(\mathrm{i}h_1 - h_2)e^{-\mathrm{i}\theta_j}\right]$ for $j = 3,4,\ldots,m$.

3.3. Computing the conformal mappings

In this paper, the integral equation (10) is solved using the MATLAB function `fbie` from [12]. In the function `fbie`, the integrals in the integral equation are discretized by the trapezoidal rule [13, 14] with n (an even positive integer) equidistant nodes in each interval J_k for $k = 1, 2, \ldots, m$. Then, by using the the Nyström method, the integral equation (10) is reduced to an $mn \times mn$ linear algebraic system which is solved iteratively using the MATLAB function `gmres`. The matrix-vector multiplication in the function `gmres` is computed efficiently using the function `zfmm2dpart` from the MATLAB toolbox `FMMLIB2D` [15]. The function `fbie` computes also the function h in (11). The complexity of the method is $O(mn \log n)$ operations.

Once the the functions $\mu(t)$ and $h(t)$ are computed at the nodes, the boundary values of function $f(z)$ can be computed at the nodes through (12). Then approximations to the values of the function $f(z)$ for $z \in G$ can be obtained using the Cauchy integral formula which can be computed numerically using the MATLAB function `fcau` from [12]. Finally the conformal mappings onto Ω_1 and Ω_2 are computed using (15) and (17) respectively.

4. Numerical Examples

In this section we consider three numerical examples. In the three examples, the presented method is used with $n = 2^{10}$ to compute the mapping function onto both canonical regions Ω_1 and Ω_2. Orthogonal grids in the unbounded region G and their images under the conformal mappings for both canonical regions Ω_1 and Ω_2 are shown in Figures 2–4. The white space in the center of the computed images corresponds to the unbounded domain in the exterior of the grids in the original region. The "dot" in the white space is $\omega(\infty)$.

Example 1 *The region G is the unbounded doubly connected region ($m = 2$) with the boundary (see Figure 2)*

$$\Gamma_1 : \quad \eta_1(t) = e^{-\mathrm{i}t},$$

$$\Gamma_2 : \quad \eta_2(t) = 2\mathrm{i} + \cos t - \mathrm{i}0.25 \sin t,$$

where $0 \le t \le 2\pi$ and $\theta = (0, \pi/2)$.

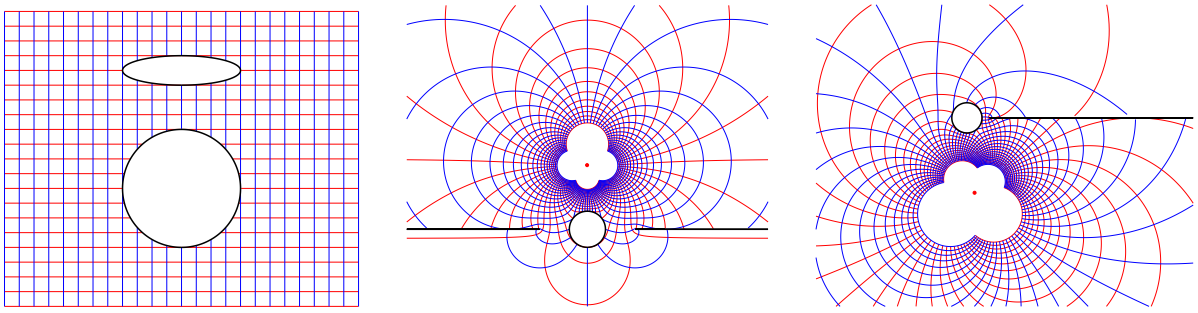

Figure 2. The original region G of Example 1 and its images to Ω_1 (center) and Ω_2 (right).

Example 2 *In the second example, the region G is the unbounded multiply connected region of connectivity $m = 7$ with $\theta = (0, \pi/2, \pi/2, \pi/4, 0, 0, 3\pi/4)$ (see Figure 3 (left)).*

Example 3 *In the third example, the region G is the unbounded multiply connected region of connectivity $m = 30$ (see Figure 4 (left)).*

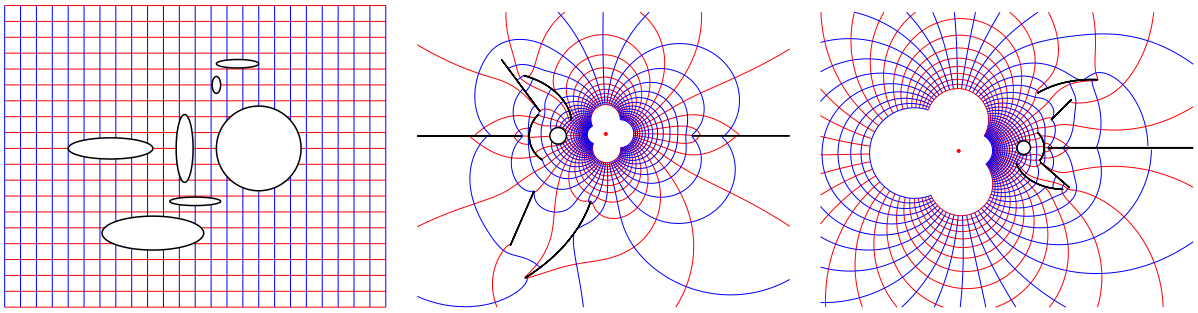

Figure 3. The original region G of Example 2 and its images to Ω_1 (center) and Ω_2 (right).

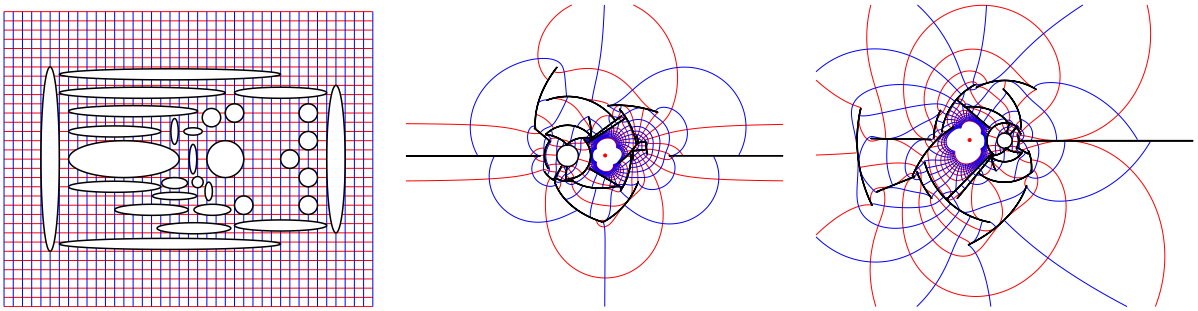

Figure 4. The original region G of Example 3 and its images to Ω_1 (center) and Ω_2 (right).

Acknowledgement

This study was supported partially through the Research Management Centre (RMC), Universiti Teknologi Malaysia (Research Grant Q.J130000.2526.16H70). This support is gratefully acknowledged.

References

[1] Schinzinger R and Laura P A 2003 *Conformal mapping: methods and applications* (New York: Dover Publications)
[2] Koebe P 1918 *Acta Math.* **41** 305–344
[3] Wegmann R 2005 *Handbook of Complex Analysis: Geometric Function Theory, Vol. 2* ed Kühnau R (Elsevier B. V.) pp 351–477
[4] Nasser M M S 2009 *SIAM J. Sci. Comput.* **31** 1695–1715
[5] Nasser M M S 2011 *J. Math. Anal. Appl.* **382** 47–56
[6] Nasser M M S 2013 *J. Math. Anal. Appl.* **398** 729–743
[7] Nasser M M S and Al-Shihri F 2013 *SIAM J. Sci. Comput.* **35** A1736–A1760
[8] Nasser M M S, Liesen J and Sète O 2016 *Comput. Methods Funct. Theory* **16** 609–635
[9] Nasser M M S 2018 *Bull. Malays. Math. Sci. Soc.* **41** 2067–2087
[10] Murid A H M and Nasser M M S 2003 *Bull. Malays. Math. Sci. Soc.* **26** 13–33
[11] Wegmann R and Nasser M M S 2008 *J. Comput. Appl. Math.* **214** 36–57
[12] Nasser M M S 2015 *Electron. Trans. Numer. Anal.* **44** 189–229
[13] Atkinson K 1997 *The Numerical Solution of Integral Equations of the Second Kind* (Cambridge: Cambridge University Press)
[14] Trefethen L N and Weideman J A 2014 *SIAM Review* **56** 385–458
[15] Greengard L and Gimbutas Z 2012 *FMMLIB2D: A MATLAB toolbox for fast multipole method in two dimensions* Version 1.2 `http://www.cims.nyu.edu/cmcl/fmm2dlib/fmm2dlib.html`